Journal of Magnetic Resonance 235 (2013) 121–129

Contents lists available at ScienceDirect

Journal of Magnetic Resonance

journal homepage: www.elsevier.com/locate/jmr

Grid-free powder averages: On the applications of the Fokker–Planck equation to solid state NMR

Luke J. Edwards [a,b], D.V. Savostyanov [b], A.A. Nevzorov [c], M. Concistrè [b], G. Pileio [b], Ilya Kuprov [b,*]

[a] Inorganic Chemistry Laboratory, Department of Chemistry, University of Oxford, South Parks Road, Oxford OX1 3QG, UK
[b] School of Chemistry, University of Southampton, Highfield Campus, Southampton SO17 1BJ, UK
[c] Department of Chemistry, North Carolina State University, 2620 Yarbrough Drive, Raleigh, NC 27695, USA

ARTICLE INFO

Article history:
Received 23 May 2013
Revised 12 July 2013
Available online 23 July 2013

Keywords:
NMR
MAS
SLE
Fokker–Planck equation
State space restriction

ABSTRACT

We demonstrate that Fokker–Planck equations in which spatial coordinates are treated on the same conceptual level as spin coordinates yield a convenient formalism for treating magic angle spinning NMR experiments. In particular, time dependence disappears from the background Hamiltonian (sample spinning is treated as an interaction), spherical quadrature grids are avoided completely (coordinate distributions are a part of the formalism) and relaxation theory with any linear diffusion operator is easily adopted from the Stochastic Liouville Equation theory. The proposed formalism contains Floquet theory as a special case. The elimination of the spherical averaging grid comes at the cost of increased matrix dimensions, but we show that this can be mitigated by the use of state space restriction and tensor train techniques. It is also demonstrated that low correlation order basis sets apparently give accurate answers in powder-averaged MAS simulations, meaning that polynomially scaling simulation algorithms do exist for a large class of solid state NMR experiments.

1. Introduction

Fokker–Planck equations that describe the time evolution of probability distributions [1,2] were first used in a magnetic resonance context in the 1970s as part of the formalism that became known as the Stochastic Liouville Equation (SLE) [3–6]. To this day SLE remains the most general relaxation theory in magnetic resonance – it is non-perturbative and works at all magnetic fields and correlation times, from extreme narrowing to the solid limit [6–8].

Initial adoption of Fokker–Planck equations was complicated by large matrix dimensions [4–6] and subsequent work had to rely heavily on sparse matrix libraries and Lanczos techniques [3], but the exponential rise in computing power in the following 40 years has removed the problem – the same calculations take just a few seconds on a contemporary workstation. Modern programming languages have also made things easier – a *Matlab* implementation of SLE in our *Spinach* library [9] takes about a hundred lines.

The advances in computing power make the Fokker–Planck formalism worth re-visiting. One particular feature that to our knowledge remains unexplored in magnetic resonance is the possibility of treating *any* spatial dynamics that can be generated by a linear operator – the formalism itself is in no way restricted to diffusion. We demonstrate below that magic angle spinning simulations in particular stand to benefit – not only is the time dependence removed from the MAS Hamiltonian (something that may already be achieved using Floquet theory [10–13]), but the need for a spherical quadrature grid also disappears: the Fokker–Planck formalism solves directly for orientation distributions and obtains the powder average in a single run. Given the amount of work that has gone into two- and three-angle spherical grids [14–21] and the computational expense of three-angle averaging, the prospect of having a *grid-free* formalism is quite attractive. Importantly, the Fokker–Planck MAS formalism contains Floquet MAS theory as a special case – when the lab space motion operator is set to be rotation and the lab space basis is chosen to be complex exponentials of the rotation angle, the equations of Floquet theory are obtained.

Another significant open question in solid state NMR is about the possibility of using state space restriction techniques [9,22,23] that only include low orders of spin correlation and result in very significant acceleration of spin dynamics simulations in liquids [9,24,25]. The Fokker–Planck formalism described below generalizes this question and makes it possible to ask whether *some correlations between spin and spatial degrees of freedom might also be redundant*. The answer to this question is shown below to be affirmative – it is demonstrated that low correlation order basis sets do provide accurate answers in powder-averaged MAS NMR simulations, although it is not entirely clear at the moment why they work so well.

* Corresponding author. Fax: +44 2380 594140.
E-mail address: i.kuprov@soton.ac.uk (I. Kuprov).

1090-7807/$ - see front matter © 2013 Elsevier Inc. All rights reserved.
http://dx.doi.org/10.1016/j.jmr.2013.07.011

2. Fokker–Planck equation for a spinning NMR sample

For a given spin system, the Liouville–von Neumann equation describing the dynamics is a linear partial differential equation for the density operator $\hat{\rho}(t)$:

$$\frac{\partial}{\partial t}\hat{\rho}(t) = -i\hat{\hat{H}}(\vec{x},t)\hat{\rho}(t) \tag{1}$$

in which $\hat{\hat{H}}(\vec{x},t)$ is the spin Hamiltonian commutation superoperator that can depend on the system orientation and/or conformation $\vec{x}$ in the lab space, which is also in general time-dependent. In deterministic cases Eq. (1) is solved directly using matrix exponentials [26,27], and in stochastic cases a relaxation superoperator is first obtained using one of the available relaxation theories [27,28]. In the cases where an average over spin system orientations or conformations is required, it is obtained by numerical or semi-analytical integration over a discrete grid of points [14–21]. This is currently the standard setting and *modus operandi* in magnetic resonance simulations.

The Fokker–Planck formalism looks at the system from a different perspective – instead of the dynamics of the density matrix $\hat{\rho}(t)$ of a specific system travelling along $\vec{x}(t)$ it considers the dynamics of the joint probability density $p(\vec{x},\hat{\rho},t)$ of systems at different lab space points $\vec{x}$ in different spin states $\hat{\rho}$. In this picture both $\vec{x}$ and $\hat{\rho}$ are time-independent coordinates and the probability density flows through their space. Notably, the special case of $p(\vec{x}\in\mathbb{R}^3,\hat{L}_+,t)$ corresponds to the MRI image of the sample. In the absence of stochastic processes, the Fokker–Planck (*aka* Smoluchowski) equation of motion for $p(\vec{x},\hat{\rho},t)$ is:

$$\frac{\partial p(\vec{x},\hat{\rho},t)}{\partial t} = -\mathrm{div}_{\hat{\rho}}[p(\vec{x},\hat{\rho},t)\,\hat{v}_{\hat{\rho}}] - \mathrm{div}_{\vec{x}}[p(\vec{x},\hat{\rho},t)\,\vec{v}_{\vec{x}}] \tag{2}$$

It has a simple physical meaning – the change in probability density at a given point is equal to the divergence of its flux. The equation is quite generic – its exact form depends on the expressions for the velocities $\hat{v}_{\hat{\rho}}$ and $\vec{v}_{\vec{x}}$ in the spin space (defined as the space of all spin operators) and the lab space (which could be bigger than $\mathbb{R}^3$ if multiple rotational and conformational degrees of freedom are considered) respectively. For a rotating NMR sample, the velocity at a point $\hat{\rho}$ in spin space is given by Eq. (1):

$$\hat{v}_{\hat{\rho}} = -i\hat{\hat{H}}(\vec{x},t)\hat{\rho} \tag{3}$$

It depends parametrically on the lab space coordinates because the spin Hamiltonian may be orientation-dependent. The lab space velocity at a specific point $\vec{x}$ may be obtained from the equations of classical mechanics describing rotational motion in three dimensions:

$$\begin{gathered}\vec{x}(t) = \exp[-i\hat{S}t]\vec{x}(0);\quad \hat{S} = \omega_S\left(n_X\hat{L}_X + n_Y\hat{L}_Y + n_Z\hat{L}_Z\right)\\ \frac{d\vec{x}(t)}{dt} = -i\hat{S}\exp[-i\hat{S}t]\vec{x}(0) = -i\hat{S}\vec{x}(t)\quad\Rightarrow\quad \vec{v}_{\vec{x}} = -i\hat{S}\vec{x}\end{gathered} \tag{4}$$

where $\left\{\hat{L}_X,\hat{L}_Y,\hat{L}_Z\right\}$ are infinitesimal generators of the rotation group and ω_S is the spinning frequency around the axis specified by a normalized $[n_X, n_Y, n_Z]$ vector. In the case of magic angle spinning $\hat{S} = \omega_S(\hat{L}_X + \hat{L}_Y + \hat{L}_Z)/\sqrt{3}$. Note that the spatial motion operator $\hat{S}$ is assumed to be classical rather than quantum mechanical, but is not restricted to rotation – the relations given in Eq. (4) hold for any deterministic motion that has a linear generator. We do assume, however, that this motion does not depend on spin.

Even with these specifics in place, solving Eq. (2) as it stands is a formidable task – it describes unitary probability flow through a space of very high dimension. Our actual target, however, is much simpler – we require the expectation value of the spin density matrix:

$$\hat{\rho}(\vec{x},t) = \int p(\vec{x},\hat{\rho},t)\hat{\rho}\,dV_{\hat{\rho}} \tag{5}$$

where $dV_{\hat{\rho}}$ is the volume element of the density matrix space. The equation of motion for the expectation value may be obtained directly:

$$\begin{aligned}\frac{\partial}{\partial t}\hat{\rho}(\vec{x},t) &= \int\left[\frac{\partial}{\partial t}p(\vec{x},\hat{\rho},t)\right]\hat{\rho}\,dV_{\hat{\rho}}\\ &= \int \mathrm{div}_{\hat{\rho}}\left[p(\vec{x},\hat{\rho},t)\left[i\hat{\hat{H}}(\vec{x},t)\hat{\rho}\right]\right]\hat{\rho}\,dV_{\hat{\rho}}\\ &\quad + \int \mathrm{div}_{\vec{x}}[p(\vec{x},\hat{\rho},t)[i\hat{S}\vec{x}]]\hat{\rho}\,dV_{\hat{\rho}}\end{aligned} \tag{6}$$

After a few straightforward vector calculus transformations, we get:

$$\frac{\partial}{\partial t}\hat{\rho}(\vec{x},t) = -i\hat{\hat{H}}(\vec{x},t)\hat{\rho}(\vec{x},t) - i\hat{S}\hat{\rho}(\vec{x},t) \tag{7}$$

In the specific case of spinning at the magic angle:

$$\frac{\partial}{\partial t}\hat{\rho}(\vec{x},t) = -i\hat{\hat{H}}(\vec{x},t)\hat{\rho}(\vec{x},t) - \frac{i\omega_S}{\sqrt{3}}\left[\hat{L}_X + \hat{L}_Y + \hat{L}_Z\right]\hat{\rho}(\vec{x},t) \tag{8}$$

where $\{\hat{L}_X,\hat{L}_Y,\hat{L}_Z\}$ are angular momentum (not spin) operators acting in lab space:

$$\begin{gathered}\hat{L}_X = -i\left(y\frac{\partial}{\partial z} - z\frac{\partial}{\partial y}\right);\quad \hat{L}_Y = -i\left(z\frac{\partial}{\partial x} - x\frac{\partial}{\partial z}\right);\\ \hat{L}_Z = -i\left(x\frac{\partial}{\partial y} - y\frac{\partial}{\partial x}\right)\end{gathered} \tag{9}$$

and ω_S is the spinning frequency. Eq. (8) is similar to the Liouville–von Neumann equation: the spin system evolution happens differently at each point in the lab space, but the additional twist is that there is now a coherent flux of spin systems between those points. The primary difference with the SLE formalism [3,6] is that the evolution prescribed by the right hand side of Eq. (8) is unitary. Note the minimal modifications that are required to adapt a working SLE code for the Fokker–Planck MAS (FPMAS) formalism: it is a simple matter of taking a different power of the lab space rotation generators. An SLE-type diffusion term may be included if necessary, and so can chemical exchange in a manner identical to the method proposed for Floquet theory [29].

It should also be noted that we did not need the very rigorous derivations *via* cumulant averages of stochastic processes that were required for the SLE [8,30] – the fact that our lab space evolution is deterministic simplifies matters a great deal because Smoluchowski equation may justifiably be used to obtain Eq. (7). There is, however, some controversy in the literature regarding the divergence operator with respect to the density matrix in Eq. (2). It is well enough defined in our opinion (spin density matrix space is finite-dimensional), but we do still provide an alternative derivation in Appendix A, which yields Eq. (7) without recourse to philosophically arguable algebraic operations.

A useful property of Eq. (8) that it has in common with SLE and inherits from the more general Eq. (2) is that distributions over lab space coordinates are a part of the formalism. This proves to be particularly convenient for the powder averaging operation that is often encountered in solid state NMR spectroscopy – if the lab space basis set is chosen to be Wigner *D*-functions:

$$\hat{H}(\Omega,t) = \sum_{lkm}\mathfrak{D}^{(l)}_{km}(\Omega)\hat{Q}^{(l)}_{km}(t),\quad \hat{\rho}(\Omega,t) = \sum_{lkm}\mathfrak{D}^{(l)}_{km}(\Omega)\hat{\sigma}^{(l)}_{km}(t) \tag{10}$$

where Ω is some parameterization of the rotation group, $\hat{Q}^{(l)}_{km}(t)$ are irreducible components of the Hamiltonian, $\hat{\sigma}^{(l)}_{km}(t)$ are irreducible components of the density matrix and $\mathfrak{D}^{(l)}_{km}(\Omega)$ are Wigner *D*-functions, then the powder average observation operation simply

amounts to calculating a scalar product of an observable operator $\hat{O}$ with $\hat{\sigma}_{00}^{(0)}(t)$:

$$\frac{1}{8\pi^2}\int_{\Omega}\mathrm{Tr}\left[\hat{O}^{\dagger}\hat{\rho}(t)\right]d\Omega=\frac{1}{8\pi^2}\sum_{lkm}\mathrm{Tr}\left[\hat{O}^{\dagger}\hat{\sigma}_{km}^{(l)}(t)\right]\int_{\Omega}\mathfrak{D}_{km}^{(l)}(\Omega)d\Omega$$
$$=\mathrm{Tr}\left[\hat{O}^{\dagger}\hat{\sigma}_{00}^{(0)}(t)\right] \tag{11}$$

In other words, the very formidable zoo of spherical grids and integration methods simply disappears and is replaced, as we shall see below, by the altogether more agreeable problem of simply storing a bigger matrix. The only adjustable parameter is the cut-off level $l_{\max}$ of the spherical expansion of the density matrix in Eq. (10), which is exactly equivalent to the spherical rank level of Lebedev type quadratures [31].

3. Numerical implementation

A numerical solution to Eq. (8) requires a matrix representation. The spin part of the problem has such a representation by construction. The lab space operators may be converted into matrices by choosing either a discrete grid of points or a basis set of continuous functions. Experiences our colleagues have had with SLE [32,33] indicate that the latter is a better choice – we shall therefore proceed to use the following variable separation ansatz:

$$\hat{H}(\vec{x},t)=\sum_{m}g_m(\vec{x})\hat{Q}_m(t)\quad\hat{\rho}(\vec{x},t)=\sum_{k}g_k(\vec{x})\hat{\sigma}_k(t) \tag{12}$$

where $g_m(\vec{x})$ are orthonormal functions of lab space coordinates, $\hat{Q}_m(t)$ are known spin operators and $\hat{\sigma}_k(t)$ are spin operators that should be solved for. The choice of the basis $\{g_m(\vec{x})\}$ creates a matrix representation for the lab space dynamics operator:

$$S_{nk}=\int g_n^{*}(\vec{x})\hat{S}g_k(\vec{x})dV_{\vec{x}}\quad\Rightarrow\quad\hat{S}g_k(\vec{x})=\sum_{n}S_{nk}g_n(\vec{x}) \tag{13}$$

and Eq. (8) becomes:

$$\sum_{k}g_k\frac{\partial\hat{\sigma}_k}{\partial t}=-i\sum_{nk}g_ng_k\hat{\hat{Q}}_n\hat{\sigma}_k-i\sum_{nk}S_{nk}g_n\hat{\sigma}_k \tag{14}$$

in which the products of lab space functions may be expressed as their linear combinations:

$$g_ng_k=\sum_{m}c_{nkm}g_m\;\Rightarrow\;c_{nkm}=\int g_n(\vec{x})g_k(\vec{x})g_m^{*}(\vec{x})dV$$
$$\sum_{k}g_k\frac{\partial\hat{\sigma}_k}{\partial t}=-i\sum_{nkm}c_{nkm}g_m\hat{\hat{Q}}_n\hat{\sigma}_k-i\sum_{nk}S_{nk}g_n\hat{\sigma}_k \tag{15}$$

Taking the scalar product on both sides with each spatial basis function $g_m(\vec{x})$ in turn yields the following system of equations:

$$\left\{\frac{\partial\hat{\sigma}_m}{\partial t}=-i\sum_{nk}c_{nkm}\hat{\hat{Q}}_n\hat{\sigma}_k-i\sum_{k}S_{mk}\hat{\sigma}_k\right\}_m \tag{16}$$

Finally, after collecting some terms, we get the following system of matrix equations:

$$\left\{\frac{\partial\hat{\sigma}_m}{\partial t}=-i\sum_{k}\left[\hat{\hat{H}}_{km}+S_{mk}\hat{\hat{E}}\right]\hat{\sigma}_k,\quad\hat{\hat{H}}_{km}=\sum_{n}c_{nkm}\hat{\hat{Q}}_n\right\}_m \tag{17}$$

where $\hat{\hat{E}}$ is the identity superoperator in the spin space. These matrix equations may be efficiently solved in the time domain using Krylov propagation [34] or in the frequency domain by calculating the Laplace transform using the Lanczos algorithm [3].

A particularly convenient practical choice for the lab space basis is Wigner *D*-functions. The associated spin operators are known as irreducible spherical tensors [3–6]. Using Eq. (10) for the spherical tensor expansion of the Hamiltonian and the density matrix, we obtain:

$$\hat{H}(\Omega,t)=\hat{H}_{\mathrm{ISO}}+\sum_{km}\mathfrak{D}_{km}^{(2)}(\Omega)\hat{Q}_{km}(t),\quad\hat{\rho}(\Omega,t)=\sum_{lkm}\mathfrak{D}_{km}^{(l)}(\Omega)\hat{\sigma}_{km}^{(l)}(t) \tag{18}$$

where $\hat{H}_{\mathrm{ISO}}$ is the orientation-independent part of the Hamiltonian, $\hat{Q}_{km}(t)$ are irreducible components of its anisotropic part and Ω is a parameterization of the rotation group, in practice usually Euler angles. Because the anisotropic Hamiltonian only contains Wigner *D*-functions of the second rank, not all structure constants are in practice required:

$$\mathfrak{D}_{km}^{(2)}(\Omega)\mathfrak{D}_{pq}^{(l)}(\Omega)=\sum_{L=|l-2|}^{l+2}\sum_{MN}C_{2,k,l,p}^{L,M}C_{2,m,l,q}^{L,N}\mathfrak{D}_{MN}^{(L)}(\Omega) \tag{19}$$

This constraint makes the evaluation of Clebsch–Gordan coefficients $C_{l_1,m_1,l_2,m_2}^{L,M}$ very affordable because simple analytical expressions exist for the special case of l1 = 2. After matrix representations are obtained, Eq. (8) acquires the following general algebraic form:

$$\frac{d}{dt}\vec{\rho}=-i\left[\mathbf{E}\otimes\mathbf{H}_{\mathrm{ISO}}+\sum_{km}\mathbf{D}_{km}^{(2)}\otimes\mathbf{Q}_{km}+\mathbf{S}\otimes\mathbf{E}\right]\vec{\rho} \tag{20}$$

where $\mathbf{E}$ is the unit matrix, $\mathbf{H}_{\mathrm{ISO}}$ is the isotropic Hamiltonian commutation superoperator matrix, $\mathbf{D}_{km}^{(2)}$ are matrix representations of right-sided Wigner *D*-function multiplication operators, $\mathbf{Q}_{km}$ are the irreducible components of the anisotropic part of the Hamiltonian commutation superoperator matrix, $\mathbf{S}$ is the spatial dynamics operator matrix and $\vec{\rho}$ is a vector representation of the density operator. In Eq. (20) matrices on the right side of Kronecker products are representations of spin operators and those on the left side are representations of operators acting on the lab space degrees of freedom.

In practical calculations, Eq. (19) is used to generate matrix representations for the Wigner *D*-function multiplication operators, Eq. (18) is used to partition the system into rank and projection blocks and the calculation is carried out forward in time using standard matrix exponentiation techniques in the Kronecker product of lab and spin spaces. SLE and FPMAS modules of our *Spinach* library [9] contain a documented open-source *Matlab* implementation of this entire section as well as source code for the practical simulation examples given below. As is frequently the case with theoretical papers and *Matlab*, the actual program code is shorter than the text of this section.

The dimension of the matrix in Eq. (17) can be large (Table 1 and Fig. 1) – it is a product of the dimensions of the spin space and the lab space. Unless special measures are taken [22,23], the former grows exponentially with the number of spins in the system and the latter grows cubically as a function of the spherical rank cut-off level $l_{\max}$. For the spin systems and Wigner *D*-function ranks required in practical simulations of common spin systems this dimension is on the brink of capability of modern computers (Table 1). An elegant way around this problem is to compute matrix–vector products prescribed by Eq. (20) without evaluating the direct products. This is always possible – given matrices $\mathbf{A}$ and $\mathbf{B}$ with elements $A_{n,m}$ and $B_{p,q}$ acting in spin space and lab space respectively, and a vector $\vec{\rho}$ that is represented in the direct product of these spaces, the matrix–vector product $\vec{\sigma}=(\mathbf{A}\otimes\mathbf{B})\vec{\rho}$ can be computed without forming $\mathbf{A}\otimes\mathbf{B}$ explicitly:

$$\sigma_{n,p}=\sum_{m,q}[A_{n,m}B_{p,q}]\rho_{m,q}=\sum_{m,q}A_{n,m}\rho_{m,q}B_{p,q} \tag{21}$$

Here elements of vectors $\vec{\sigma}$ and $\vec{\rho}$ depend on both spin indices n, m and lab space indices p, q. In matrix notation this equation is simply $\boldsymbol{\sigma}=\mathbf{A}\boldsymbol{\rho}\mathbf{B}^{\mathrm{T}}$, where $\boldsymbol{\sigma}$ and $\boldsymbol{\rho}$ are the vectors $\vec{\sigma}$ and $\vec{\rho}$ reshaped into

Table 1
Liouvillian dimension and non-zero count statistics for glycine, alanine and sucrose spin systems in a proton-decoupled ^{13}C pulse-acquire 2.0 kHz MAS NMR simulation using Floquet, FPMAS and tensor train FPMAS formalisms.

System	Liouvillian matrix statistics							
		Single-point	Floquet with 2-angle grid[a]	Floquet with 3-angle grid[b]	FPMAS, full	FPMAS, reduced[c]	TT-FPMAS[d], full	TT-FPMAS[d], reduced[e]
Glycine (^{13}C, ^{15}N), Wigner rank 23, Fourier rank 20, complete basis	*dim*	64	2624 (194 points)	2624 (4656 points)	1,179,136	165,816	64 ⊗ 18,424 (26 terms)	9 ⊗ 18,424 (7 terms)
	nnz	0.2 k	38 k (194 points)	38 k (4656 points)	76 M	13 M	456 k	455 k
Alanine, (^{13}C, ^{15}N), Wigner rank 23, Fourier rank 20, complete basis	*dim*	256	10,496 (194 points)	10,496 (4656 points)	4,716,544	571,144	256 ⊗ 18,424 (26 terms)	31 ⊗ 18,424 (7 terms)
	nnz	1.4 k	290 k (194 points)	290 k (4656 points)	567 M	79 M	464 k	456 k
Sucrose (^{13}C), Wigner rank 23, Fourier rank 20, 3-spin order basis.	*dim*	6571	269,411 (194 points)	269,411 (4656 times)	121,964,104	26,991,160	6,571 ⊗ 18,424 (26 terms)	1,465 ⊗ 18,424 (7 terms)
	nnz	49 k	7.1 M (194 points)	7.1 M (4656 points)	>45 G	3.1 G	672 k	507 k

[a] Rank 23 Lebedev quadrature [31].
[b] Rank 23 GSQ quadrature [17].
[c] Conservation law screening [39] followed by zero track elimination [22] followed by path tracing [39].
[d] Tensor train formalism [36].
[e] Conservation law screening [39].

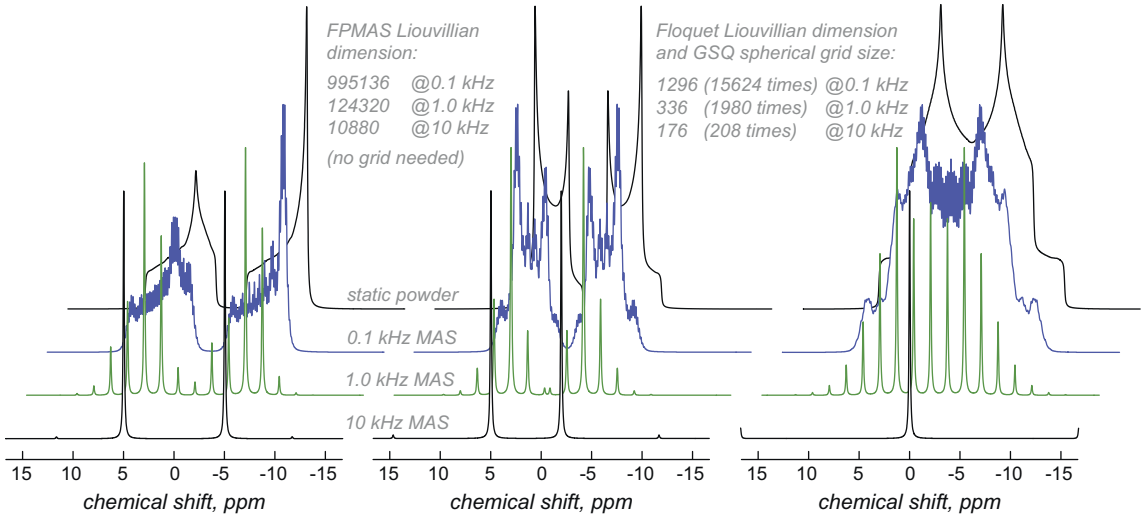

Fig. 1. Results and matrix dimension statistics for basic CSA, dipolar and quadrupolar powder patterns calculated for different sample spinning rates with Floquet and Fokker–Planck formalism. The following algorithm parameters were used, selected in such a way as to achieve numerical convergence of the resulting spectra to approximately 10^{-3} relative accuracy: (10 kHz trace) maximum Fourier rank 5, GSQ grid rank 7 for Floquet simulation, maximum Wigner function rank 7 for Fokker–Planck simulation; (1.0 kHz trace) maximum Fourier rank 10, GSQ grid rank 17 for Floquet simulation, maximum Wigner function rank 17 for Fokker–Planck simulation; (0.1 kHz trace) maximum Fourier rank 40, GSQ grid rank 35 for Floquet simulation, maximum Wigner function rank 35 for Fokker–Planck simulation. Three-angle GSQ grids [17] on the Floquet side and full Wigner function basis sets on the Fokker–Planck side were chosen to provide an apples-to-apples comparison: two-angle averages would have sufficed for the simulations shown above, but we have chosen to use the most general simulation case for the comparison.

spin-by-lab matrices. Such reshaping does not require any permutations of the arrays stored in memory, it only switches the way that these arrays are seen: for instance, $\boldsymbol{\sigma}$ is a matrix with spin and lab indices being row and column indices and $\vec{\sigma}$ is a vector stored along a single multi-index $i = (n-1)P + p$, where P denotes the number of possible values for p. With this in place, the matrix–vector multiplication on the right hand side of Eq. (17) can be performed as a sum of two-sided matrix multiplications that avoid the calculation of the very large $\mathbf{A} \otimes \mathbf{B}$ matrices. Because Krylov time propagation algorithms only require matrix–vector multiplication, this means that the time propagation problem can likewise be solved at a much reduced memory cost. More generally, the structure of the matrix in Eq. (20) is a simple example of a tensor train – an object that generalizes, from the numerical linear algebra point of view, the MPS/DMRG methods proposed initially in quantum physics [35]. Very efficient algorithms exist for manipulating tensor trains without unfolding the direct products [35,36].

The primary advantage of Eq. (21) is in the memory requirements – for storage purposes the product of the numbers of non-zeros in **A** and **B** matrices is effectively replaced by their sum. This is illustrated in the two rightmost columns of Table 1 – the memory requirements for the storage of a tensor train representation of an FPMAS Liouvillian are about the same as those of single-orientation Floquet run and in the case of sucrose are actually smaller. For sucrose (a 12-spin system for ^{13}C MAS NMR purposes) this proves to be critical – the sparse matrix representation of the FPMAS Liouvillian crashes our best supercomputer, while the tensor train representation fits into the L3 cache of a single CPU. Given the ubiquity of direct product sums in magnetic resonance theory, it is quite clear that tensor train representations of spin operators should be used more widely in simulations.

4. Relation to Floquet theory

Floquet theory, as applied to NMR spectroscopy, is a special case of Eq. (7). This relationship becomes clear when the fairly arbitrary lab space motion permitted in the right hand side of Eq. (7) is constrained to be uniform rotation around a specific axis:

$$\frac{\partial}{\partial t}\hat{\rho}(\varphi,t) = -i\hat{\hat{H}}(\varphi)\hat{\rho}(\varphi,t) + \omega_S\frac{\partial}{\partial\varphi}\hat{\rho}(\varphi,t) \tag{22}$$

where the orientation is now described by an angle φ, the Hamiltonian superoperator is assumed to only depend on that angle, $\partial/\partial\varphi$ is the rotation generator and ω_S is the spinning rate. Because the angle φ is now periodic, the following variable separation ansatz may be used without loss of generality:

$$\hat{\rho}(\varphi,t) = \sum_n \hat{\rho}_n(t)\exp(in\varphi) \quad \hat{H}(\varphi) = \sum_k \hat{H}_k\exp(ik\varphi) \tag{23}$$

where the Fourier indices n and k run over all integers. After the substitution is performed, Eq. (22) becomes:

$$\sum_n \exp(in\varphi)\left[\frac{\partial}{\partial t}\hat{\rho}_n(t)\right] = \sum_{kn}\exp\left[i(k+n)\varphi\right]\left[-i\hat{H}_k\hat{\rho}_n(t)\right] + \sum_n \exp(in\varphi)[in\omega_S\hat{\rho}_n(t)] \tag{24}$$

After rotating the summation indices of the double sum and equating the coefficients of the same Fourier factors, we obtain:

$$\left\{\frac{\partial}{\partial t}\hat{\rho}_m(t) = -i\sum_n \hat{H}_{m-n}\hat{\rho}_n(t) + im\omega_S\hat{\rho}_m(t)\right\}_m \tag{25}$$

which is identical to the Floquet theory equations for the Fourier components of the density matrix [10–13]. This completes the proof and has a side effect of providing a rather neat alternative derivation for the Floquet MAS formalism.

The primary advantage of Eq. (7) over Eq. (25) is that three-angle powder averages are built into the FPMAS formalism – as demonstrated in Eq. (11), there is no need for a spherical quadrature grid. Another advantage is greater variety of spatial dynamics models that the right hand side of Eq. (7) can accommodate – the $\hat{S}$ term may be set to any linear operator, including also translation and diffusion [3]. That having been said, Floquet theory does hold its own in one significant category – the ease of parallelization: it is quite straightforward to distribute several thousand independent Floquet calculations for different system orientations to different nodes of a cluster, but considerably harder (though not impossible [37]) to parallelize a single-trajectory simulation of the kind required by the FPMAS formalism.

5. Incomplete basis sets

A general observation in liquid state magnetic resonance spectroscopy is that the complete basis set in the spin operator space is rarely necessary because amplitudes of highly correlated spin states are kept low by the inevitable presence of relaxation processes [23,38]. Very fast simulation algorithms are obtained when unpopulated spin states are dropped from the basis set [25,39]. The same is not in general true for solid state NMR, where dense networks of strong interactions populate high correlation orders in milliseconds – the left panel of Fig. 2 demonstrates this for alanine during a proton-decoupled MAS pulse-acquire experiment on ^{13}C at a single randomly selected orientation. From the immediate appearance of the graph one might conclude that state space restriction approximation is not applicable to solid state NMR – all spin correlation orders get populated quickly to levels that clearly cannot be ignored.

We would like to report a surprising observation though – as the right panel of Fig. 2 demonstrates, effective amplitudes of multi-spin correlations are much reduced when a powder average of the density matrix is taken at each point in the trajectory. In practice that means that *even though highly correlated states are active in each individual crystallite, the spectrometer coil does not feel their presence in the powder*. For the purposes of simulating spinning powder-averaged NMR spectra the high spin correlations can therefore be ignored, implying that polynomially scaling algorithms of the same kind as were developed for liquids [9,22,23,39] could be possible, at least for pulse-acquire MAS NMR experiments. A quick look at the simulation results in a simple spin system (Fig. 3) confirms this – the simulated spectra with complete and truncated basis sets are essentially the same across the range of spinning rates. Another example, along with experimental data, is given in Fig. 4 for uniformly ^{13}C and ^{15}N labeled tryptophan – a large spin system not at present accessible to a complete basis set simulation. Even though three-spin and higher correlations are clearly present in the quantum trajectory of each individual crystallite, accurate answers are still obtained when they are ignored. This phenomenon might be general – a similar finding was reported in the recent work on spin diffusion by the Emsley group [25,40,41], who also found that powder averaging

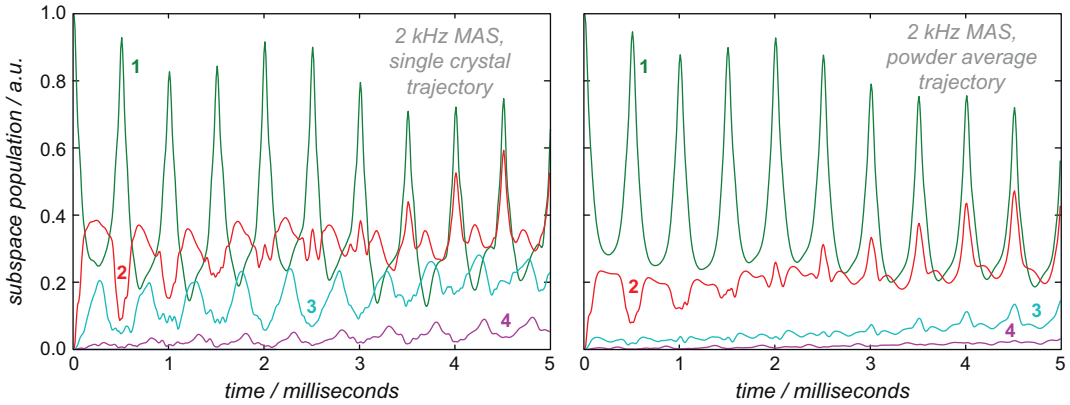

Fig. 2. Spin system trajectory analysis during the detection period of ^{13}C pulse-acquire MAS NMR experiment on ^{13}C,^{15}N-labeled alanine under proton decoupling. Left panel – spin correlation order dynamics in a single crystallite: the state space is filled completely with significant population in four-spin orders. Right panel – spin correlation order dynamics in a powder-averaged density matrix: orientation averaging appears to reduce the effective level of spin correlation in the trajectory, the populations of three- and four-spin orders are significantly reduced.

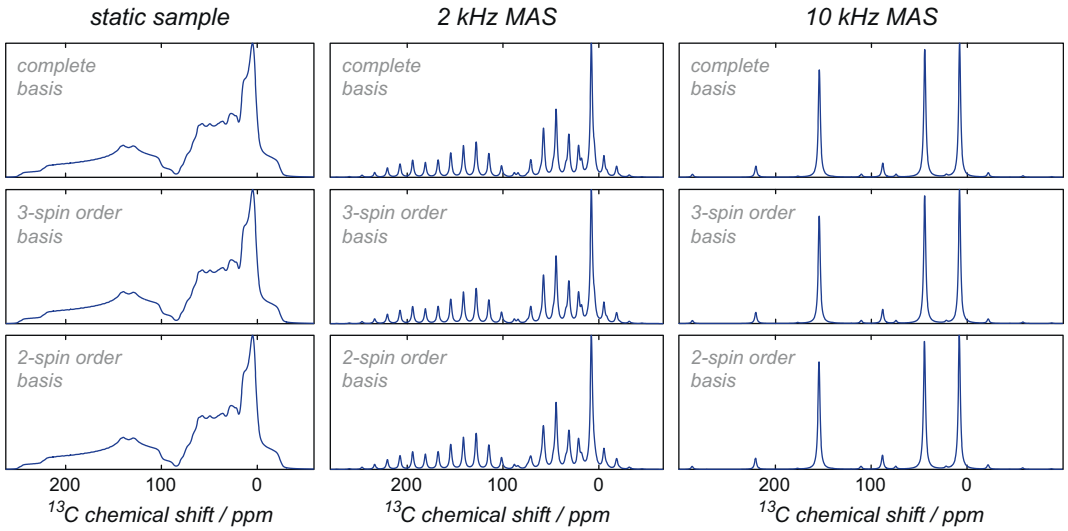

Fig. 3. Basis set convergence of restricted state space calculations of ^{13}C pulse-acquire MAS NMR spectra of ^{13}C,^{15}N-labeled alanine powder under proton decoupling. The difference between the full state space (top row) and reduced state spaces (middle and bottom rows) is minor – the maximum relative difference from the exact simulation is $\sim 10^{-3}$ for three-spin order basis set and $\sim 10^{-2}$ for the two-spin order basis set. This level of accuracy is unexpected because three- and four-spin correlations do get populated (see Fig. 2) during the system evolution.

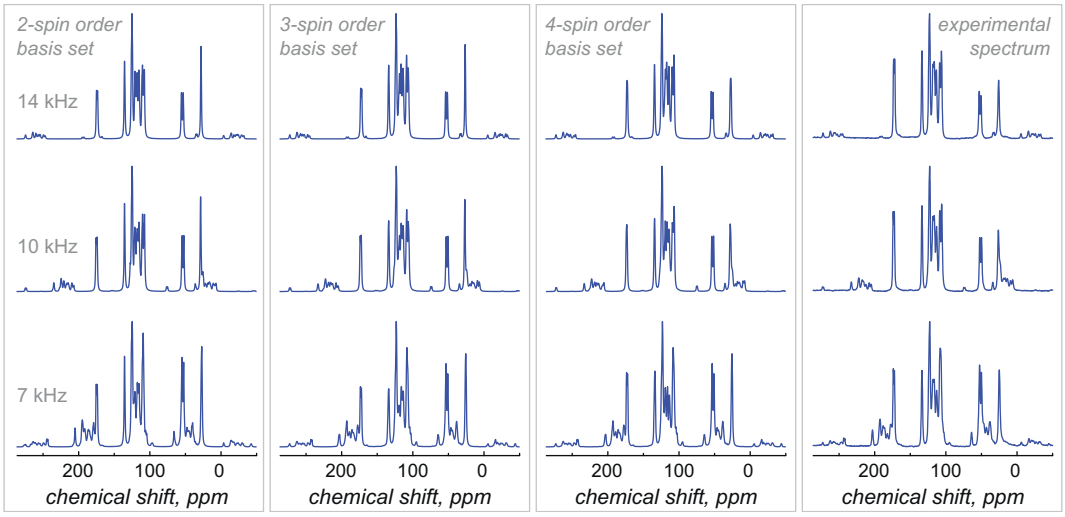

Fig. 4. Basis set convergence and comparison with the experimental data for the restricted state space calculations of ^{13}C pulse-acquire MAS NMR spectra of uniformly ^{13}C,^{15}N-labeled tryptophan powder under proton decoupling. For the purposes of the simulation, Cartesian coordinates of the tryptophan amino acid were extracted from the Cambridge Structural Database, the coordinates of the hydrogen atoms were re-optimized using DFT B3LYP/cc-pVTZ method [46–48] *in vacuo*. Isotropic chemical shifts were read off from the experimental data and chemical shielding tensor anisotropies were estimated with GIAO B3LYP/cc-pVTZ method [49] and used without further fitting. *J*-couplings were estimated using the same method with a decontracted cc-pVTZ basis set augmented with tight functions in the nuclear region. All DFT calculations were performed in Gaussian 09. Experimental ^{1}H-decoupled CP-MAS spectra were recorded for a powdered sample of uniformly ^{13}C,^{15}N-labeled D,L-tryptophan (Cambridge Isotope Labs) packed in a 4 mm zirconia rotor. A 400 MHz Varian Infinity Plus NMR spectrometer was used. Spectra were acquired with three different values of the spinning rate: 14, 10, 7 kHz (top to bottom). SPINAL decoupling was used with a proton pulse duration of 6.5 μs corresponding to a nutation frequency of 75 kHz. Cross-polarization conditions were adjusted for each spinning rate value; for the 10 kHz trace a contact time of 2.5 ms and a nutation frequency of 50 kHz for protons and 40 kHz for carbon were used.

mysteriously improved the accuracy of a low correlation order basis set that was not, from common sense expectations, supposed to work at all.

A qualitative explanation as to why reduced basis sets suffice for the simulation of powder MAS spectra may be obtained by inspection of the effect that the powder averaging has on the spin system propagator of a stationary sample. For the free induction decay $f(t)$ at time t of a system that has started evolution in a state $|\hat{\rho}(0)\rangle$ and is detected at the state $|\hat{\sigma}\rangle$, we have:

$$f(t) = \frac{1}{8\pi^2}\int_{\Omega}\left[\langle\hat{\sigma}|\exp\left(-i\hat{\hat{H}}(\Omega)t\right)|\hat{\rho}(0)\rangle\right]d\Omega \tag{26}$$

Using the irreducible spherical tensor expansion for the Hamiltonian:

$$\hat{H}(\Omega) = \sum_{lkm}\hat{Q}^{(l)}_{km}\mathfrak{D}^{(l)}_{km}(\Omega) \tag{27}$$

and a Taylor series expansion for the matrix exponential, we get:

$$\begin{aligned} f(t) &= \frac{1}{8\pi^2}\int_{\Omega}\left[\left\langle\hat{\sigma}\left|\sum_{n=0}^{\infty}\frac{(-it)^n}{n!}\left(\sum_{lkm}\hat{Q}^{(l)}_{km}\mathfrak{D}^{(l)}_{km}(\Omega)\right)^n\right|\hat{\rho}(0)\right\rangle\right]d\Omega \\ &= \frac{1}{8\pi^2}\sum_{n=0}^{\infty}\frac{(-it)^n}{n!}\left[\left\langle\hat{\sigma}\left|\int_{\Omega}\left(\sum_{lkm}\hat{Q}^{(l)}_{km}\mathfrak{D}^{(l)}_{km}(\Omega)\right)^n d\Omega\right|\hat{\rho}(0)\right\rangle\right] \end{aligned} \tag{28}$$

Table 2
Floquet and Fokker–Planck simulation run time statistics for glycine, alanine and sucrose spin systems in a proton-decoupled ^{13}C pulse-acquire 2.0 kHz MAS NMR simulation.

System	Run time (s)						
	Single crystal	Floquet with 2-angle grid[a]	Floquet with 3-angle grid[b]	FPMAS, full	FPMAS, reduced[c]	TT-FPMAS[d], full	TT-FPMAS[d], reduced[e]
Glycine (^{13}C,^{15}N), Wigner rank 23, Fourier rank 20, complete basis	2.60×10^{-1}	5.04×10^{1}	1.21×10^{3}	6.25×10^{3}	9.21×10^{2}	3.58×10^{4}	4.20×10^{3}
Alanine, (^{13}C,^{15}N), Wigner rank 23, Fourier rank 20, complete basis	2.89×10^{0}	5.60×10^{2}	1.34×10^{4}	6.14×10^{4}	5.69×10^{3}	1.84×10^{5}	1.82×10^{4}
Sucrose (^{13}C), Wigner rank 23, Fourier rank 20, 3-spin order basis	5.27×10^{2}	1.02×10^{5}	2.45×10^{6}	$>10^{7}$	6.24×10^{5}	3.39×10^{6}	5.83×10^{5}

[a] Rank 23 Lebedev quadrature [31].
[b] Rank 23 GSQ quadrature [17].
[c] Conservation law screening [39] followed by zero track elimination [22] followed by path tracing [39].
[d] Tensor train formalism [36].
[e] Conservation law screening [39].

The initial and the detection state in MAS NMR contain only single-spin correlations and the question is therefore narrowed to which correlation orders are populated and subsequently returned into the single-spin order subspace by the following superoperators:

$$\frac{1}{8\pi^2}\int_{\Omega}\left(\sum_{lkm}\hat{\hat{Q}}^{(l)}_{km}\mathcal{D}^{(l)}_{km}(\Omega)\right)^{n}d\Omega=\frac{1}{8\pi^2}\int_{\Omega}\left(\sum_{lkm}\hat{\hat{P}}^{(l,n)}_{km}\mathcal{D}^{(l)}_{km}(\Omega)\right)d\Omega \quad (29)$$

The right hand side of this equation follows from the fact that Wigner D-functions are a complete basis set in the space of all continuous functions of Ω. Due to the restrictions on the physical nature of spin interaction operators only $l \leqslant 2$ ranks appear in $\hat{\hat{Q}}^{(l)}_{km}$, but $\hat{\hat{P}}^{(l,n)}_{km}$ operators can in general have any l rank.

The presence of the full spherical average is now revealed to be the critical factor – most Wigner D-functions integrate to zero and only the terms multiplied by $\mathfrak{D}^{(0)}_{00}(\Omega)$ survive the powder integration:

$$\frac{1}{8\pi^2}\int_{\Omega}\left(\sum_{lkm}\hat{\hat{P}}^{(l,n)}_{km}\mathfrak{D}^{(l)}_{km}(\Omega)\right)d\Omega=\hat{\hat{P}}^{(0,n)}_{00} \quad (30)$$

The remaining operators $\hat{\hat{P}}^{(0,n)}_{00}$ are complicated linear combinations of powers of $\hat{\hat{Q}}^{(l)}_{km}$ – we could not find a way to express them compactly, but what is clear from Eq. (30) is that a massively smaller number of spin operators is present in the effective powder average propagator compared to the single crystal propagator – just one per Taylor series term, compared to the full three-index sum from Eq. (29) for the single crystal case. The zero spherical rank and projection quantum numbers of $\hat{\hat{P}}^{(0,n)}_{00}$ also explain why the dynamics mostly stays in the low correlation order subspace. These are qualitative arguments, however – a more rigorous and quantitative analysis has thus far defeated our attempts. It should also be noted that the observations reported in this section apply in equal measure to both Floquet and Fokker–Planck description of MAS NMR – the simulation results are identical.

6. Numerical performance

The price for the generality of the motion model and for the removal of spherical grids in the Fokker–Planck formalism is paid in matrix dimensions. Those are astronomical, even by the liberal standards of Floquet theory (Table 1), but the ability to work with large matrices has much improved in recent years – it is currently possible to handle spin Liouvillians with dimensions well in excess of 10^7, particularly if Lanczos type algorithms [3], sparse libraries [42,43] and state space restriction methods [9,22,23] are used.

One saving grace is that the matrices involved are always very sparse – this has been known for a long time [29,43], but we recently also demonstrated that the fraction of non-zeros in spin Hamiltonians drops exponentially as the system size is increased [37]. Another saving grace is the above noted tensor train format for the Liouvillian storage [36]. It does not reduce the amount of multiplications needed, but shrinks the memory footprint of the simulation by several orders of magnitude. It becomes essential for the simulation of systems with more than about five spins.

Because FPMAS solves for the three-angle orientational average, a set of three-angle GSQ grids (which descend from Lebedev grids and whose spherical rank is equivalent to FPMAS Wigner rank [17]) are used with Floquet theory to provide the apples-to-apples performance comparison given in Table 2. The conclusion is that there is no significant consistent performance difference between the two theories – an order of magnitude or so can be seen in favor of either Floquet or Fokker–Planck, the winner depending on the system. When state space restriction techniques are used (*e.g.* only the +1 coherence level is necessary for pulse-acquire simulations, only longitudinal states are populated on ^{15}N, *etc.*), FPMAS formalism is marginally faster.

7. Conclusions

We propose a Fokker–Planck type formalism for the simulation of magic angle spinning NMR experiments. The two primary advantages over the *status quo* are that sample spinning is treated as just another time-independent interaction term in the Liouvillian and that powder averages are obtained in a single run – there is no spherical quadrature grid. Relaxation theory with any algebraically linear diffusion operator may be easily adopted from the closely related Stochastic Liouville Equation formalism by adding a diffusion term to the right hand side of Eq. (7). We have also demonstrated that the Fokker–Planck MAS formalism contains the NMR version of Floquet theory as a special case.

The elimination of the spherical grid comes at the cost of increased matrix dimensions, but we show that this can be mitigated by the use of state space restriction and tensor train techniques. We have also demonstrated that low correlation order basis sets apparently give accurate answers in powder MAS simulations, meaning that polynomially scaling simulation algorithms do exist for a large class of solid state NMR experiments.

Acknowledgments

We are grateful to Jean-Nicolas Dumez, Jack Freed, Meghan Halse, Eva Meirovitch, Malcolm Levitt and Shimon Vega for very

useful discussions. The project is supported by EPSRC (EP/H003789/1, EP/J013080/1).

Appendix A

This section gives an alternative derivation of Eq. (7) that avoids using a divergence operator with respect to the density matrix. Here we also start from the Liouville–von Neumann equation for the trajectory of an individual spin system with the Hamiltonian that depends parametrically on some time-dependent lab space coordinates $\vec{x}(t)$:

$$\frac{d\hat{\rho}(t)}{dt} = -i\hat{\hat{H}}(\vec{x}(t))\hat{\rho}(t) \tag{31}$$

Because the motion described by $\vec{x}(t)$ is deterministic, we may label the individual trajectories by the value of $\vec{x}(t)$ at time zero – we will refer to the individual coordinate trajectories as $\vec{x}(t|x_0)$ and to the individual spin system trajectories as $\hat{\rho}(t|x_0)$. With these labels in place, the equation of motion for each individual spin system trajectory becomes:

$$\frac{d\hat{\rho}(t|x_0)}{dt} = -i\hat{\hat{H}}(\vec{x}(t|x_0))\hat{\rho}(t|x_0) \tag{32}$$

This approach is distinct from the stochastic case [8,30], where the labeling of trajectories by their starting points would not have been possible. To ensure convergence of the various integrals below, we would also require the range of $\vec{x}(t)$ to be finite.

As per the topic of the paper, we are not interested in individual trajectories, but rather in the evolution of the entire field of density matrices $\hat{\rho}(\vec{x},t)$ at each lab space coordinate point $\vec{x}$. Such a field may be obtained by taking an integral over the individual trajectories:

$$\hat{\rho}(\vec{x},t) = \int P(\vec{x},t|\vec{x}_0,0)\hat{\rho}(t|x_0)P(\vec{x}_0,0)d\vec{x}_0 \tag{33}$$

where $P(\vec{x},t|\vec{x}_0,0)$ is the conditional probability density for the lab space coordinates and $P(\vec{x}_0,0)$ is the probability density of the initial conditions. Because the lab space motion is deterministic, $P(\vec{x},t|\vec{x}_0,0)$ is given simply by

$$P(\vec{x},t|\vec{x}_0,0) = \delta(\vec{x} - \vec{x}(t|x_0)) \tag{34}$$

In the most general case, the coordinates on which the spin Hamiltonian depends would be a set of canonical coordinates and momenta (usually denoted $\{q_i\}$ and $\{p_i\}$). The conditional probability density may then be recognized as the classical density in phase space $\rho(\vec{q},\vec{p},t)$ subject to the initial condition $\rho(\vec{q},\vec{p},0) = \delta(\vec{q}-\vec{q}_0)\delta(\vec{p}-\vec{p}_0)$.

In order to find the equation of motion for $\hat{\rho}(\vec{x},t)$, we shall differentiate the integral of Eq. (33), weighted with an arbitrary continuous operator $\hat{f}(\vec{x})$ that will be required for the application of the fundamental lemma of the calculus of variations [44] later on:

$$\begin{aligned}\frac{d}{dt}\int \hat{\rho}(\vec{x},t)\hat{f}(\vec{x})d\vec{x} &= \int \frac{\partial\hat{\rho}(\vec{x},t)}{\partial t}\hat{f}(\vec{x})d\vec{x} \\ &= \iint \left[\frac{\partial P(\vec{x},t|\vec{x}_0,0)}{\partial t}\hat{\rho}(t|x_0) + P(\vec{x},t|\vec{x}_0,0)\frac{\partial\hat{\rho}(\vec{x}_0,t)}{\partial t}\right] \\ &\times P(\vec{x}_0,0)\hat{f}(\vec{x})d\vec{x}_0 d\vec{x}\end{aligned} \tag{35}$$

Because the lab space motion is classical, the time derivative of the probability density may be obtained from the Liouville equation [45]:

$$\begin{aligned}\frac{\partial P(\vec{x},t|\vec{x}_0,0)}{\partial t} &= -[(\nabla_{\vec{p}}P(\vec{x},t|\vec{x}_0,0))\cdot(\nabla_{\vec{q}}H) - (\nabla_{\vec{p}}H)\cdot(\nabla_{\vec{q}}P(\vec{x},t|\vec{x}_0,0))] \\ &= \Gamma P(\vec{x},t|\vec{x}_0,0)\end{aligned} \tag{36}$$

where H is the classical Hamiltonian of the lab space dynamics. We may thus write that:

$$\iint \frac{\partial P(\vec{x},t|\vec{x}_0,0)}{\partial t}\hat{\rho}(t|x_0)P(\vec{x}_0,0)\hat{f}(\vec{x})d\vec{x}_0 d\vec{x} = \int \Gamma\hat{\rho}(\vec{x},t)\hat{f}(\vec{x})d\vec{x} \tag{37}$$

The second term under the double integral in Eq. (35) may be simplified by inserting the right hand side of the Liouville–von Neumann equation in the place of the time derivative:

$$\begin{aligned}&\iint \left[P(\vec{x},t|\vec{x}_0,0)\frac{\partial\hat{\rho}(t|x_0)}{\partial t}\right]P(\vec{x}_0,0)\hat{f}(\vec{x})d\vec{x}_0 d\vec{x} \\ &= -i\iint \left[P(\vec{x},t|\vec{x}_0,0)\hat{\hat{H}}(\vec{x}(t|x_0))\hat{\rho}(t|x_0)\right]P(\vec{x}_0,0)\hat{f}(\vec{x})d\vec{x}_0 d\vec{x} \\ &= -i\int \left[\hat{H}(\vec{x})\hat{\rho}(\vec{x},t)\right]\hat{f}(\vec{x})d\vec{x}\end{aligned} \tag{38}$$

where Eq. (34) was used to switch $\vec{x}(t|x_0)$ arguments to $\vec{x}$. We can now insert the result into the fundamental lemma of the calculus of variations [44]:

$$\int \left[\frac{\partial\hat{\rho}(\vec{x},t)}{\partial t} - \Gamma\hat{g}(\vec{x},t) + i\hat{\hat{H}}(\vec{x})\hat{\rho}(\vec{x},t)\right]\hat{f}(\vec{x})d\vec{x} = 0 \quad \forall\hat{f}(\vec{x}) \tag{39}$$

to conclude that the equation of motion for the field of density matrices is:

$$\frac{\partial\hat{\rho}(\vec{x},t)}{\partial t} = -i\hat{\hat{H}}(\vec{x})\hat{\rho}(\vec{x},t) + \Gamma\hat{\rho}(\vec{x},t) \tag{40}$$

in general agreement with Eq. (7). The last remaining task – to derive the expression for the lab space motion generator Γ – is accomplished in the way identical to the procedure given in Eq. (4).

References

[1] A.D. Fokker, Die mittlere Energie rotierender elektrischer Dipole im Strahlungsfeld, Ann. Phys. 348 (1914) 810–820.
[2] M. Planck, Über einen Satz der statistischen Dynamik und seine Erweiterung in der Quantentheorie, Sitzungsber. Kön. Preuss. Akad. Wiss. (1917) 324–341.
[3] G. Moro, J.H. Freed, Calculation of ESR-spectra and related Fokker–Planck forms by the use of the Lanczos-algorithm, J. Chem. Phys. 74 (1981) 3757–3773.
[4] R.P. Mason, J.H. Freed, Estimating microsecond rotational correlation times from lifetime broadening of nitroxide electron-spin resonance-spectra near rigid limit, J. Phys. Chem. 78 (1974) 1321–1323.
[5] C.F. Polnaszek, G.V. Bruno, J.H. Freed, ESR line shapes in slow-motional region – anisotropic liquids, J. Chem. Phys. 58 (1973) 3185–3199.
[6] J.H. Freed, G.V. Bruno, C.F. Polnaszek, Electron spin resonance line shapes and saturation in slow motional region, J. Phys. Chem. 75 (1971) 3385–3399.
[7] A.A. Nevzorov, Orientational and motional narrowing of solid-state NMR lineshapes of uniaxially aligned membrane proteins, J. Phys. Chem. B 115 (2011) 15406–15414.
[8] A.A. Nevzorov, J.H. Freed, Spin relaxation by dipolar coupling: from motional narrowing to the rigid limit, J. Chem. Phys. 112 (2000) 1413–1424.
[9] H.J. Hogben, M. Krzystyniak, G.T.P. Charnock, P.J. Hore, I. Kuprov, Spinach – a software library for simulation of spin dynamics in large spin systems, J. Magn. Reson. 208 (2011) 179–194.
[10] I. Scholz, J.D. van Beek, M. Ernst, Operator-based Floquet theory in solid-state NMR, Solid State Nucl. Magn. Reson. 37 (2010) 39–59.
[11] M. Leskes, P.K. Madhu, S. Vega, Floquet theory in solid-state nuclear magnetic resonance, Prog. Nucl. Magn. Reson. Spectrosc. 57 (2010) 345–380.
[12] A.D. Bain, R.S. Dumont, Introduction to Floquet theory: the calculation of spinning sideband intensities in magic-angle spinning NMR, Concepts Magn. Reson. 13 (2001) 159–170.
[13] A. Schmidt, S. Vega, The Floquet theory of nuclear magnetic resonance spectroscopy of single spins and dipolar coupled spin pairs in rotating solids, J. Chem. Phys. 96 (1992) 2655–2680.
[14] B. Stevensson, M. Edén, Efficient orientational averaging by the extension of Lebedev grids via regularized octahedral symmetry expansion, J. Magn. Reson. 181 (2006) 162–176.
[15] M. Edén, Computer simulations in solid-state NMR. III. Powder averaging, Concepts Magn. Reson. 18 (2003) 24–55.
[16] A. Ponti, Simulation of magnetic resonance static powder lineshapes: a quantitative assessment of spherical codes, J. Magn. Reson. 138 (1999) 288–297.
[17] M. Edén, M.H. Levitt, Computation of orientational averages in solid-state NMR by Gaussian spherical quadrature, J. Magn. Reson. 132 (1998) 220–239.
[18] M. Bak, N.C. Nielsen, Repulsion, a novel approach to efficient powder averaging in solid-state NMR, J. Magn. Reson. 125 (1997) 132–139.

[19] S.J. Varner, R.L. Vold, G.L. Hoatson, An efficient method for calculating powder patterns, J. Magn. Reson. 123 (1996) 72–80.
[20] D. Wang, G.R. Hanson, A new method for simulating randomly oriented powder spectra in magnetic resonance: the Sydney opera house (SOPHE) method, J. Magn. Reson. 117 (1995) 1–8.
[21] M.J. Mombourquette, J.A. Weil, Simulation of magnetic resonance powder spectra, J. Magn. Reson. 99 (1992) 37–44.
[22] I. Kuprov, Polynomially scaling spin dynamics II: further state-space compression using Krylov subspace techniques and zero track elimination, J. Magn. Reson. 195 (2008) 45–51.
[23] I. Kuprov, N. Wagner-Rundell, P.J. Hore, Polynomially scaling spin dynamics simulation algorithm based on adaptive state-space restriction, J. Magn. Reson. 189 (2007) 241–250.
[24] A. Karabanov, A. van der Drift, L.J. Edwards, I. Kuprov, W. Kockenberger, Quantum mechanical simulation of solid effect dynamic nuclear polarisation using Krylov–Bogolyubov time averaging and a restricted state-space, Phys. Chem. Chem. Phys. 14 (2012) 2658–2668.
[25] M.C. Butler, J.N. Dumez, L. Emsley, Dynamics of large nuclear-spin systems from low-order correlations in Liouville space, Chem. Phys. Lett. 477 (2009) 377–381.
[26] M.H. Levitt, Spin Dynamics: Basics of Nuclear Magnetic Resonance, Wiley, 2008.
[27] R.R. Ernst, G. Bodenhausen, A. Wokaun, Principles of Nuclear Magnetic Resonance in One and Two Dimensions, Oxford University Press, 1987.
[28] A. Abragam, The Principles of Nuclear Magnetism, Clarendon, 1961.
[29] P. Hazendonk, A.D. Bain, H. Grondey, P.H.M. Harrison, R.S. Dumont, Simulations of chemical exchange lineshapes in CP/MAS spectra using Floquet theory and sparse matrix methods, J. Magn. Reson. 146 (2000) 33–42.
[30] J.H. Freed, in: L.T. Muus, P.W. Atkins (Eds.), Electron Spin Relaxation in Liquids, Plenum, 1972. pp. 188–190.
[31] V.I. Lebedev, D.N. Laikov, Quadrature formula for the sphere of 131-th algebraic order of accuracy, Dokl. Akad. Nauk SSSR 366 (1999) 741–745.
[32] A.E. Stillman, G.P. Zientara, J.H. Freed, Variational method and the stochastic-Liouville equation. 2. ESR spectral simulation via finite-elements, J. Chem. Phys. 71 (1979) 113–118.
[33] J.H. Freed, J.B. Pedersen, The theory of chemically induced dynamic nuclear polarization, Adv. Magn. Reson. 8 (1976) 2–81.
[34] D.J. Tannor, Introduction to Quantum Mechanics: A Time-dependent Perspective, University Science Books, 2007.
[35] U. Schollwock, The density-matrix renormalization group in the age of matrix product states, Ann. Phys. 326 (2011) 96–192.
[36] I.V. Oseledets, Tensor-train decomposition, SIAM J. Sci. Comput. 33 (2011) 2295–2317.
[37] L.J. Edwards, I. Kuprov, Parallel density matrix propagation in spin dynamics simulations, J. Chem. Phys. 136 (2012).
[38] A. Karabanov, I. Kuprov, G.T.P. Charnock, A. van der Drift, L.J. Edwards, W. Köckenberger, On the accuracy of the state space restriction approximation for spin dynamics simulations, J. Chem. Phys. 135 (2011).
[39] H.J. Hogben, P.J. Hore, I. Kuprov, Strategies for state space restriction in densely coupled spin systems with applications to spin chemistry, J. Chem. Phys. 132 (2010).
[40] J.-N. Dumez, M.E. Halse, M.C. Butler, L. Emsley, A first-principles description of proton-driven spin diffusion, Phys. Chem. Chem. Phys. 14 (2012) 86–89.
[41] J.-N. Dumez, M.C. Butler, L. Emsley, Numerical simulation of free evolution in solid-state nuclear magnetic resonance using low-order correlations in Liouville space, J. Chem. Phys. 133 (2010).
[42] M. Veshtort, R.G. Griffin, SPINEVOLUTION: a powerful tool for the simulation of solid and liquid state NMR experiments, J. Magn. Reson. 178 (2006) 248–282.
[43] R.S. Dumont, S. Jain, A. Bain, Simulation of many-spin system dynamics via sparse matrix methodology, J. Chem. Phys. 106 (1997) 5928–5936.
[44] I.M. Gelfand, S.V. Fomin, Calculus of Variations, Prentice-Hall, 1963.
[45] R.C. Tolman, The Principles of Statistical Mechanics, Dover, 1979.
[46] A.D. Becke, A new mixing of Hartree-Fock and local density-functional theories, J. Chem. Phys. 98 (1993) 1372–1377.
[47] T.H. Dunning, Gaussian-basis sets for use in correlated molecular calculations. 1. The atoms boron through neon and hydrogen, J. Chem. Phys. 90 (1989) 1007–1023.
[48] C.T. Lee, W.T. Yang, R.G. Parr, Development of the Colle–Salvetti correlation-energy formula into a functional of the electron-density, Phys. Rev. B 37 (1988) 785–789.
[49] F. London, Théorie quantique des courants interatomiques dans les combinaisons aromatiques, J. Phys. Radium 8 (1937) 397–409.